Index sensing characteristics of the plasmonic sensor based on metal-insulator-metal waveguide-coupled structure*

GUO Jian-ping (郭健平)[1,2]**, **ZHU Jia-hu** (朱家胡)[1], and **HUANG Xu-guang** (黄旭光)[1]

1. Laboratory of Nanophotonic Functional Materials and Devices, South China Normal University, Guangzhou 510006, China

2. School of Physics and Telecommunication Engineering, South China Normal University, Guangzhou 510006, China

(Received 30 April 2013)

A plasmonic refractive index sensor based on metal-insulator-metal (MIM) waveguide-coupled structure is proposed and demonstrated in this paper. The physical mechanism of the device is deduced, and the finite difference time domain (FDTD) method is employed to simulate and study its index sensing characteristics. Both analytic and simulated results show that the resonant wavelength of the sensor has a linear relationship with the refractive index of material under sensing. Based on the relationship, the refractive index of the material can be obtained from the detection of the resonant wavelength. The results show that the sensitivity of the sensor can exceed 1600 nm/RIU, and it can be used in chemical and biological detections.

Document code: A **Article ID:** 1673-1905(2013)05-0321-4

DOI 10.1007/s11801-013-3081-8

Since the first surface plasmon resonance (SPR) integrated optical sensor was described in late 1980s[1], various integrated optical SPR sensors using slab waveguide, channel waveguide and even more complex waveguide structure have been demonstrated[2-6], but for most of conventional waveguides, the diffraction limit of light poses a significant challenge to the miniaturization and ultra-density integration of optical circuits[7].

Plasmonic waveguides, based on surface plasmons polaritons (SPPs) propagating at the metal-dielectric interfaces, have been considered as one of promising candidates to overcome the classical diffraction limit for their ability to guide and manipulate light at deep subwavelength scales[7,8]. Compared with other types of sensors, the plasmonic waveguide integrated sensor has an inherent advantage to achieve high integration[8,9].

Recently several plasmonic sensors have been investigated. Lu et al[10] designed a nanosensor based on Fano resonance in the double-nanoresonator system. Wu[11] and Chen[12] presented the experimental demonstration for a refractive index sensor based on the interference of two SPP waves in the slit metallic structure. In this paper, a simple and compact plasmonic sensor based on metal-insulator-metal (MIM) waveguide-coupled structure is proposed. The physical mechanism of the device is deduced. The finite difference time domain (FDTD) method with a perfectly matched layer (PML) absorbing boundary condition is employed to simulate and study its properties. The simulation results show that the sensitivity of the sensor is about 1000 nm/RIU, which is as good as other highly sensitive SPR sensors, and it may be used in chemical and biological detections[13,14].

The proposed sensor structure is shown in the inset of Fig.1. It is constructed by a subwavelength MIM waveguide side-coupled to a cavity which is filled with the material under sensing (MUS). The waveguide is divided into two segments acting as input port and output port separated by a metal barrier, where w and w' stand for the widths of the waveguide and cavity, and L and L_{bar} are the lengths of the cavity and the barrier, respectively. w_{gap} denotes the gap distance between the waveguide and the MUS cavity. The metal here is assumed to be silver whose frequency-dependent complex relative permittivity is characterized by the Drude model[15], and the dielectric in the waveguide is assumed to be SiO_2 with a refractive index n=1.47. The MUS cavity can be filled up with gaseous or liquid MUS with different methods. Gaseous MUS can be simply diffused into the cavity based on gas diffusion force in vacuum circumstance. Liquid MUS can be filled up into the cavity using nano-filling technique based on capillarity attraction[16]. Firstly, part of the inner surface of the cavity is wetted by the liquid MUS. Secondly, the liquid penetrates into the cavity by the capillarity pumping effect, which makes the cavity full of the liquid MUS.

* This work has been supported by the National Natural Science Foundation of China (No.61275059), the Excellent Young Teachers Program of South China Normal University (No.2012KJ002), and the "973" Project (No.2011CBA00200).

** E-mail: guojpgz@163.com

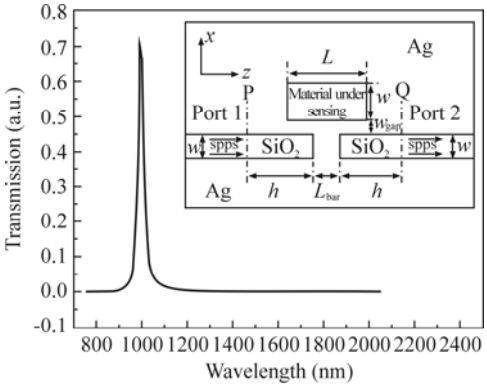

Fig.1 Typical transmission spectrum of the plasmonic refractive index sensor (The inset is the two-dimensional schematic diagram with *L*=300 nm, *h*=150 nm and w_{gap}=20 nm.)

When a fundamental transverse magnetic (TM) mode is excited at the input port, part of the waves will be reflected at the front surface of metal barrier, while the other part of the waves can be coupled into the cavity due to the small width of the gap. The forward and backward waves in the cavity are almost completely reflected at the silver-air interfaces at both ends until a standing wave is formed, and then would be coupled forward into the output port. Therefore, the structure operates like a Fabry-Perot resonance cavity.

Define $\Delta\varphi$ to be the total phase delay per round-trip in the MUS cavity, which is

$$\Delta\phi=k(\omega)\times 2L+2\psi_{\mathrm{r}}\ , \tag{1}$$

where $k(\omega)$ is the angular wavenumber of the waves in the cavity at frequency ω, L is the length of the cavity, and ψ_{r} is the phase shift of the beam reflected at one end of the cavity. A standing wave would exit only when the following resonant condition is satisfied:

$$\Delta\phi = m\times 2\pi\ (m=1,\ 2,\ 3\cdots)\ , \tag{2}$$

where positive integer m is the number of antinodes of the standing SPPs wave. Using the relation[17] of

$$\mathrm{Re}[k(\omega)] = 2\pi n_{\mathrm{eff}}/\lambda\ , \tag{3}$$

and combining Eqs.(1) and (2), the resonant wavelengths λ_m are finally given as

$$\lambda_m = \frac{2n_{\mathrm{eff}}L}{m-\psi_{\mathrm{r}}/\pi}\ (m=1,\ 2,\ 3\cdots)\ , \tag{4}$$

where n_{eff} is the real part of the effective index in the MUS cavity, whose value can be obtained by solving the dispersion relation of the fundamental TM mode in an MIM waveguide[15]:

$$\tanh(-\frac{\mathrm{i}k_{z1}}{2}w') = -\frac{\varepsilon_{\mathrm{m}}k_{z2}}{\varepsilon_{\mathrm{MUS}}k_{z1}}\ , \tag{5}$$

where k_{z1} and k_{z2} are defined by momentum conservations as

$$\begin{cases} k_{z1}^2 = \varepsilon_{\mathrm{MUS}}k_0^2 - \beta^2 \\ k_{z2}^2 = \varepsilon_{\mathrm{m}}k_0^2 - \beta^2 \end{cases}\ , \tag{6}$$

where $\beta=\beta_{\mathrm{R}}+\mathrm{i}\beta_{\mathrm{I}}$ is the complex propagation constant, $\varepsilon_{\mathrm{MUS}}=n_{\mathrm{MUS}}^2$ and ε_{m} are the dielectric constants of the MUS and metal, respectively, and $k_0=2\pi/\lambda$ is the wavenumber of light in vacuum. The real part of the effective index in the MUS cavity n_{eff} is given by $n_{\mathrm{eff}}=\beta_{\mathrm{R}}/k_0$. The relationship between n_{eff} and n_{MUS} can be calculated based on Eqs.(5) and (6). If the MUS cavity is filled up with different materials whose refractive indices are known and the resonant wavelength of the transmission spectrum is detected, the calibration curve of the sensor can be obtained as the resonant wavelength versus the refractive index. For an unknown material, if the transmission spectrum is detected, its refractive index can be got by using the calibration curve. Thus a plasmonic sensor device can be achieved.

In order to investigate the characteristics of the plasmonic sensor, the FDTD method is employed to calculate the transmission spectra of the proposed structure. In the following FDTD simulations, the grid sizes in both x and z directions are chosen to be 5 nm. PML absorbing boundary condition is used at all boundaries of the simulation domain. Power monitors are set at the positions of P and Q to detect the incident power of P_{in} and the transmitted power of P_{out}, respectively. During the simulation, the width of the waveguide w and the length of the barrier L_{bar} are fixed to be 50 nm and 100 nm, respectively, while other parameters are changable. The width of the waveguide is much smaller than the wavelength so that only the fundamental SPPs mode can be supported[18].

At first, we can assume that the MUS cavity is filled with air, whose refractive index is 1. For the structure with the parameters of L=300 nm, h=150 nm, w'=50 nm and w_{gap}=20 nm, the transmission spectrum of the structure is shown in Fig.1. It can be seen that there is a resonant wavelength at 997.3 nm with a maximum transmission about 69.9%.

For a non-coupling air-filled MIM waveguide with the width of 50 nm, its effective index n_{eff} can be calculated to be 1.41 for incident wavelength of 997.3 nm based on Eqs.(5) and (6). Because the cavity length is at the order of the wavelength, L_{pen1} and L_{pen2} must be taken into account, which means the surface plasmon waves penetrating into the left and right sides of the resonance cavity respectively. The effective cavity length of a microcavity is given by the sum of the optical length of cavity and penetration depths on both sides. Thus Eq.(4) may be modified to be

$$\lambda_m = \frac{2L_{\mathrm{eff}}}{m-\psi_{\mathrm{r}}/\pi}\ (m=1,\ 2,\ 3\cdots)\ , \tag{7}$$

where $L_{\mathrm{eff}}=n_{\mathrm{eff}}L+L_{\mathrm{pen1}}+L_{\mathrm{pen2}}$, and the penetration depth can be calculated by the relationship[19] as

$$L_{\mathrm{pen}} = \frac{\lambda\psi_{\mathrm{r}}}{4\pi}\ . \tag{8}$$

When the obtained effective cavity length is substituting to Eq.(7), the phase shift at the wavelength λ=997.3 nm can be determined to be ψ_r=0.078π for m=2. Similarly, other resonance wavelengths can be calculated by substituting m with other values. If the length of MUS cavity is chosen properly, there would be only one transmittance extremum in the wavelength range from 700 nm to 1800 nm of interest, which may be helpful to improve the performance of the sensor.

Now the cavity can be filled with different materials whose refractive indices have been known. Fig.2(a) shows the simulated results of transmission spectra of the sensor structure for different refractive indices while the geometric parameters of sensor are kept as the same as those in Fig.1. The resonant wavelengths show a red shift as the refractive index n is increased. When the refractive index is increased from 1.0 to 1.6, the resonant wavelength shifts from 997.3 nm to 1602.1 nm. Fig.2(b) displays the linear relationship between the resonant wavelength and the refractive index. It can be seen that the shift of resonant wavelength as a function of the refractive index is equal to 996.6 nm per refractive index unit (RIU), which is moderate compared with other SPR on-chip platforms[14].

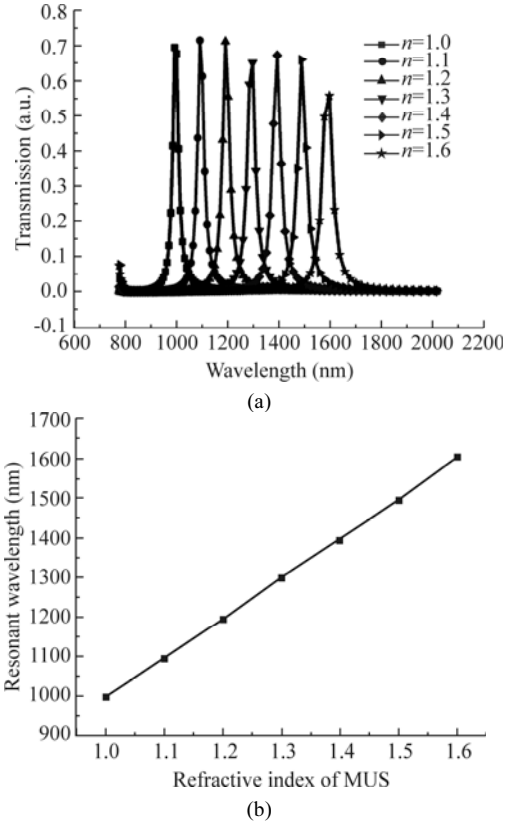

Fig.2 (a) Simulated reflection spectra of the sensor for different refractive indices n_{MUS} with L=300 nm and w'=50 nm; (b) The resonant wavelength versus the refractive index of the MUS

When the MUS cavity is filled with an unknown material, if the resonant wavelength of the sensor is measured to be 1250 nm, from Fig.2(b), the refractive index n_{MUS} is obtained to be 1.261. At the same time, according to Eqs.(5) and (7), substituting L=300 nm and resonant wavelength λ=1250 nm for m=2, the refractive index n_{MUS} is calculated to be 1.263 when assuming the phase shift to be unchanged as ψ_r=0.078π. Therefore, the theoretical analysis fairly agrees with the simulation result.

Fig.3 displays the resonant wavelength of the sensor as a function of the MUS cavity refractive index n_{MUS} for different cavity widths and lengths. Fig.3(a) shows that the change rate of dλ/dn for the narrower MUS cavity is higher than that for the wider one. It can be seen more clearly in Fig.3(b). The sensitivity of the sensor drops from 1010 nm/RIU for 50 nm-width cavity structure down to 840 nm/RIU for 100 nm-width cavity one. What is more, the sensitivity drops much faster at narrower cavity while just changes slightly at wider ones, which is obvious especially when the width exceeds 100 nm. Fig.3(c) and (d) illustrate the resonant wavelength and the sensitivity of the sensor as a function of the refractive index of the MUS for different cavity lengths. The sensitivity of the sensor increases with the increase of the cavity length. So the performance of the sensor can be enhanced by lengthening and narrowing the MUS cavity. For example, the sensitivity of the sensor with the cavity L=550 nm and w'=50 nm is 1687 nm/RIU, which is twice of that with the cavity L=300 nm and w'=150 nm (798 nm/RIU). However, narrowing down the MUS cavity can increase the difficulty in fabrication and make it more challenging to inject the MUS into the cavity. At the same time, the simulated result reveals that the transmission loss is significantly large when L>1000 nm[18]. On all accounts, the suitable geometric parameters of the MUS cavity should be chosen to obtain a desired sensitivity.

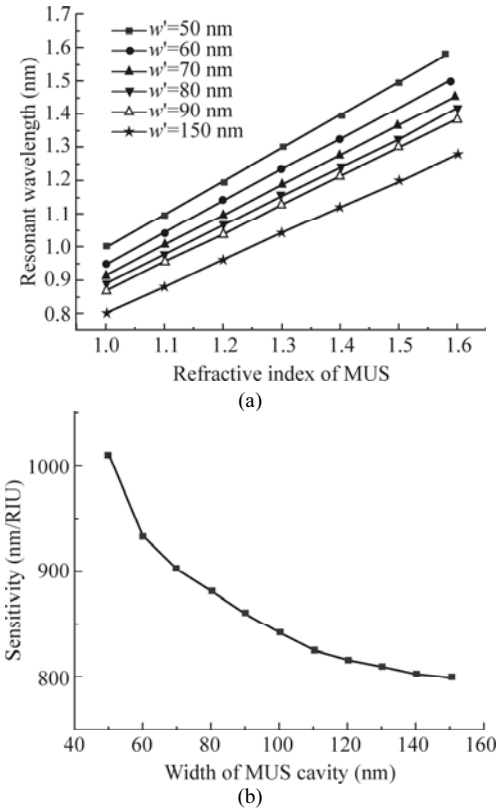

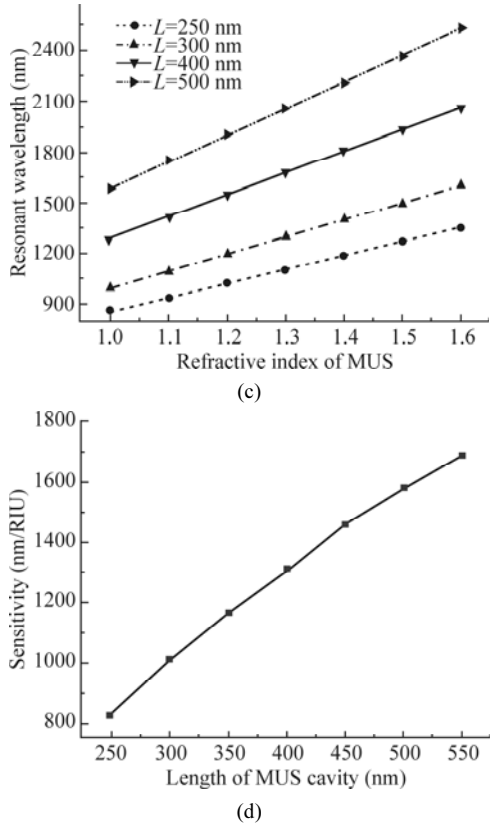

Fig.3 Resonant wavelength of the transmission spectrum versus the refractive index *n* of the MUS cavity (a) with different widths and the fixed length of 300 nm and (c) with different lengths and the fixed width of 50 nm; The sensitivity of the sensor (b) with fixed cavity length of 300 nm versus the cavity width and (d) with fixed cavity width of 50 nm versus the cavity length

In conclusion, a plasmonic refractive index sensor based on MIM waveguide-coupled structure is introduced and demonstrated. The resonant wavelength of the sensor has a linear relationship with the refractive index of MUS. The sensitivity of the sensor can be improved by lengthening and narrowing the MUS cavity. The simulation results show that the sensitivity of the sensor can exceed 1600 nm/RIU if properly designed. The simple structure has a compact size with hundreds of nanometers in width and length. Thus the device can be an important step to a fully integrated surface plasmon lab-on-chip solution, which means that it may be used in high-resolution chemical and biological detections.

Acknowledgements

The authors thank Professor Sheng Lan for helpful discussions.

References

[1] H. J. M. Kreuwel, P. V. Lambeck, J. V. Gent and T. J. A. Popma, Proc. SPIE **789**, 218 (1987).
[2] R. D. Harris and J. S. Wilkinson, Sensors and Actuators B: Chemical **29**, 261 (1995).
[3] C. R. Lavers and J. S. Wilkinson, Sensors and Actuators B: Chemical **22**, 475 (1994).
[4] R. Levy, A. Peled and S. Ruschin, Sensors and Actuators B: Chemical **119**, 20 (2006).
[5] J. Liu, B. Chen and H. Yang, Journal of Optoelectronics·Laser **22**, 1821 (2011). (in Chinese)
[6] Y. Yuan, L. Ding and Z. Guo, Sensors and Actuators B: Chemical **157**, 240 (2011).
[7] W. Barnes, A. Dereus and T. Ebbsen, Nature **424**, 824 (2003).
[8] D. Gramotnev and S. Bozhevolnyi, Nature Photonics **4**, 83 (2010).
[9] E. Ozbay, Science **311**, 189 (2006).
[10] H. Lu, X. Liu, D. Mao and G. Wang, Optics Letters **37**, 3780 (2012).
[11] X. Wu, J. Zhang, J. Chen, C. Zhao and Q. Gong, Refractive Index Sensor based on Surface-plasmon Interference, Optics Letters **34**, 392 (2009).
[12] W. Chen, C. Jian-Jun, T. Wei-Hua and X. Jing-Hua, Chinese Physics Letters **29**, 127304 (2012).
[13] M. E. Stewart, C. R. Anderton, L. B. Thompson, J. Maria, S. K. Gray, J. A. Rogers and R. G. Nuzzo, Chem. Rev. **108**, 494 (2008).
[14] D.-J. Lee, H.-D. Yim, S.-G. Lee and B.-H. O, Optics Express **19**, 19895 (2011).
[15] Z. Han, E. Forsberg and S. He, IEEE Photonics Technology Letters **19**, 91 (2007).
[16] A.Y. Vorobyev and C. Guo, Applied Physics Letters **94**, 224102 (2009).
[17] X.-S. Lin and X.-G. Huang, Optics Letters **33**, 2874 (2008).
[18] J. Dionne, L. Sweatlock, H. Atwater and A. Polman, Plasmon Slot Waveguides: Towards Chip-scale Propagation with Subwavelength-scale Localization, Physical Review B **73**, 035407 (2006).
[19] A. Dodabalapur, L. J. Rothberg, R. H. Jordan, T. M. Miller, R. E. Slusher and J. M. Phillips, Journal of Applied Physics **80**, 6954 (1996).